Heliyon 10 (2024) e24242

Contents lists available at ScienceDirect

Heliyon

journal homepage: www.cell.com/heliyon

Research article

Green synthesis of copper ions nanoparticles functionalized with rhamnolipid as potential antibacterial agent for pathogenic bacteria

Fera Faridatul Habibah [a], Wa Ode Sri Rizki [a], Atthar Luqman Ivansyah [b], Dea Indriani Astuti [c], Rukman Hertadi [a,*]

[a] Biochemistry Research Division, Faculty of Mathematics and Natural Sciences, Institute Technology Bandung, Bandung, Indonesia
[b] Analytical Chemistry Research Division, Faculty of Mathematics and Natural Sciences, Institute Technology Bandung, Bandung, Indonesia
[c] Microbial Biotechnology Research Division, School of Life Science and Technology, Institute Technology Bandung, Bandung, Indonesia

ARTICLE INFO

Keywords:
Copper/rhamnolipid-based nanoparticles
Antibacterial agents
Green synthesis
Pathogenic bacteria

ABSTRACT

Copper-based nanoparticles possess broad-spectrum antibacterial activity against both gram-positive and gram-negative bacteria, making them a cost-effective alternative to other metal-based nanoparticles. The development of eco-friendly copper based nanopaticles using biodegradable and non-toxic biosurfactants, such as rhamnolipid is being explored in this study. In the present study, Cu(I)-rhamnolipid nanoparticles (Cu(I)-Rl Nps) was prepared by coprecipitation method. The structural analysis by using FTIR and XRD techniques revealed that Cu(I)-Rl Nps was successfully produced, as indicated by the detectable of ionic and covalent-coordinations bond between rhamnolipid and Cu(I) ions. Further analysis using TEM, PSA and ZPA suggest that the resulted Cu(I)-Rl Nps have spherical shape with the diameter range of 141.7–536.3 nm and the surface charge of −30 mV, respectively. The antibacterial activity of Cu(I)-Rl Nps surpassed that of the copper-based nanoparticles, free-state Cu(I) ions and rhamnolipid, which was determined by MIC/MBC methods. The Cu(I)-Rl Nps inhibition to the growth of *Bacillus subtilis* ATCC 6633 (Gram-positive) gave the MIC/MBC values of 19/19 μg/mL, while the copper-based nanoparticles, free-state Cu(I) ions and rhamnolipid gave the MIC/MBC value of 1250/2500, 1250/1250, 62/62 μg/mL, respectively. Further test on *Escherichia coli* ATCC 6538 (Gram-negative) showed that the Cu(I)-Rl Nps gave the MIC/MBC value of 78/78 μg/mL, while the copper-based nanoparticles, free-state Cu(I) ions and rhamnolipid gave the MIC/MBC value of 2500/2500, 2500/2500, 2000/2000 μg/mL, respectively. The increased antibacterial activity of Cu(I)-Rl Nps was due to the synergistic effects between Cu(I) and rhamnolipid.

1. Introduction

An Antibacterial agents play a key role in limiting the growth of pathogenic bacteria. Due to contaminated food, water, medical devices, and invasion of healthy tissues, pathogenic bacteria can cause disease in the human body [1]. Infection with pathogenic bacteria can have adverse effects on human health and even result in death. Since the discovery of the first antibiotic (penicillin) by

* Corresponding author.
E-mail address: rhertadi@itb.ac.id (R. Hertadi).

https://doi.org/10.1016/j.heliyon.2024.e24242
Received 31 August 2023; Received in revised form 19 November 2023; Accepted 4 January 2024
Available online 6 January 2024

Alexander Fleming in 1928, the process of managing and treating infections caused by pathogenic bacteria has achieved greater efficacy, thereby improving human health [2]. However, along with the discovery of several traditional antimicrobial agents such as antibiotics, antiseptic and disinfectants currently available on the market, it has been reported that many pathogenic bacteria have evolved to develop resistance to these materials, especially during pandemic.

Antibacterial resistance occurs through several pathways, such as enzyme modification or inactivation, reduced intracellular accumulation, changes in target sites of antimicrobial agents, and resistance to antibiotics through the spread of resistant genes [3]. Therefore, microorganisms have numerous strategies to counteract the effects of antibacterial actions. This approach increases the severity of the infection and makes the pathogenicity of resistant bacteria more challenging to treat. Numerous strategies have been implemented to combat antibacterial resistance. One of these strategies involves the discovery and development of novel antibacterial agents.

Among these, one of the strategy includes the use of nanomaterials as novel antibacterial agents which have toxic properties against various strains of bacteria. In recent years, metal-based nanoparticles have been studied intensively for their application as antibacterial agents. It is because metal-based nanoparticles do not bind to a specific receptor on the bacterial cell membrane hence, it is impossible for bacteria to build resistance to such a treatment and expands the spectrum of treatments with antibacterial activity [4]. Several mechanisms are proposed to explain the antibacterial activity of metal-based nanoparticles, including ion leaching, ion dissolution, and reactive oxygen species (ROS) generations [5,6]. This particular method induces damage to cellular membranes and walls, consequently interfering with crucial metabolic pathways for the sustenance of bacterial cells. Therefore, this allows for their utilization in the biomedical field as antibacterial agent. In addtions, other studies have utilized metal nanoparticles (e.g., TiO_2) in combination with UV-C light to disinfect large surfaces via a Photocatalytic Oxidation Conveyor (PCOC) system [7]. This method combines the interaction of photons from UV-C light with metal oxide nanoparticles to produce hydroxy radicals which have an impact on the disinfection process.

Copper is one of the precursors utilized in the synthesis of metal-based nanoparticles. Copper-based nanoparticles have been shown to possess exceptional antimicrobial properties [8]. However, they exhibit lower effectiveness compared to silver or zinc-based nanoparticles, necessitating higher concentrations of copper to achieve comparable results [9]. Nevertheless, copper is a more cost-effective option than other nanometals, making it a practical component of nanomaterial for enhancing antibacterial efficacy.

Commonly used techniques for synthesizing metal-based nanoparticles involve chemical reduction and microemulsion-based methods [10,11]. These methods employ surfactants as reducing and capping agents to prevent particle agglomeration and promote uniform dispersion in solution. The adsorption of surfactants onto metal nanoparticle surfaces is the key event in stabilizing these complexes [12]. In green nanoparticle synthesis, the use of non-toxic reagents as reducing and stabilizing agents is crucial. As a result, attempts have been made to replace synthetic surfactants with biodegradable surfactants produced by microorganisms (biosurfactant) in the production of metal-based nanoparticles [13].

Rhamnolipids are an environmentally friendly glycolipid biosurfactant known for their biodegradability and low toxicity [14]. They have also been found to exhibit antimicrobial properties against a broad spectrum of both Gram-positive and Gram-negative bacteria, including *Streptococcus pneumonia, Staphylococcus epidermidis, Salmonella typhi, Klebsiella pneumonia*, and *Escherichia coli* [15]. In addition, it has been reported that the combination of a rhamnolipid with several other materials, including silver metal ions and chitosan polymers, increases the stability and antibacterial activity of the mixture in comparison to their individual components [16,17]. Rhamnolipid acts as a reducing agent and capping agent to preserve the stability of nanoparticle dispersion in solution. This property is feasible due to the presence of hydroxy groups within the rhamnolipid structure.

Based on these data, we developed a novel nanoparticle by combining copper ion nanoparticles with rhamnolipids (Cu(I)-Rl Nps). The coprecipitation technique under basic conditions in NaOH solution was used to synthesize Cu(I)-Rl Nps. The rhamnolipid acting as both a reducing agent and capping agent. To better understand the characteristics of the synthesized nanoparticles, a number of analyses were carried out, including structure and component analysis with Fourier-transform infrared spectroscopy (FTIR), X-ray diffraction (XRD), scanning electron microscopy with energy dispersive X-ray analysis (SEM-EDS), morphological analysis with transmission electron microscopy (TEM), surface charge analysis with a zeta potential analyzer (ZPA), and particle size distribution analysis using a particles size analyzer (PSA). To determine the stability of Cu(I)-Rl Nps dispersion in solution, a stability test was carried out by measuring the absorbance of Cu(I)-Rl Nps dispersion with UV–Vis Spectrophotometry.

In addition, the synergistic effects of Cu(I)-Rl Nps antibacterial activity were analyzed by determining the inhibition zone with the diffusion well sensitivity test, and determining the minimum inhibitory concentration (MIC) and minimum bactericidal concentration (MBC) by employing *Staphylococcus aureus* ATCC 6538, *Bacillus subtilis* ATCC 6633, *Escherichia coli* ATCC 6539, and *Salmonella typhi* ATCC 8939 as bacterial models to represent the different effects on Gram-negative and Gram-positive bacteria. As demonstrated by the findings of this study, Cu(I)-Rl Nps have potential to be used as antibacterial agent which has the potential to be utilized in multiple industrial sectors.

2. Materials and methods

2.1. Chemicals, reagents, and bacterial strains

Rhamnolipid (from *Pseudomonas aeruginosa*) were purchased from AGAE Technologies (USA). Copper (II) nitrate trihydrate. ($Cu(NO_3).4H_2O$), and sodium hydroxide (NaOH) were of analytical grade and purchased from Merck, Singapore. The bacterial strains used for the antibacterial assay in this research included *Staphylococcus aureus* ATCC 6538, *Bacillus subtilis* ATCC 6633, *Escherichia coli* ATCC 6539, and *Salmonella typhi* ATCC 8939, which were obtained from the School of Pharmacy, Bandung Institute of Technology,

Indonesia.

2.2. Methods

2.2.1. Synthesis of the nanoparticles

Minor adjustments were made to the synthetic approach proposed by Hertadi et al. (2020) for producing copper ions-based Nps and Cu(I)-Rl Nps using coprecipitation method [18]. The copper metal ions from $Cu(NO_3)_2.3H_2O$ acted as the core of the nanoparticles and as an oxidizing agent, while the rhamnolipid functioned as a reducing and capping agent for the copper nanoparticles. The molar ratio used in this synthesis is 3:1 (rhamnolipid:$Cu(NO_3)_2.3H_2O$). In the initial step of the synthesis, 0.6 g of rhamnolipid were dissolved in 0.2 % (w/v) NaOH solution to obtain a rhamnolipid solution. Next, 100 mM $Cu(NO_3)_2.3H_2O$ solution was added dropwise to the rhamnolipid solution. The mixture was stirred using a magnetic stirrer for 15 min at room temperature. Subsequently, the mixture was heated to 100 °C for 8 h to aid in the metal-ion reduction process. Changes in the color of the solution from blue to green indicated the reduction of the Cu^{2+} ion by rhamnolipids had taken place. The Cu(I)-Rl Nps suspension was cooled at room temperature for ±15 min and centrifuged at 8000 rpm for 15 min at 4 °C. After the washing and drying process, the solid obtained was determined to be Cu(I)-Rl Nps. Copper ions-based Nps were obtained in the same manner as that of Cu(I)-Rl Nps, except with the use of deionized water instead of the rhamnolipid. The suspension of copper ions-based Nps was cooled at room temperature for ±15 min and centrifuged at 8000 rpm for 15 min at 4 °C. After the washing and drying process, the solid obtained was determined to be copper ions-based Nps.

2.2.2. Characterization of the nanoparticles

The structure of the nanoparticles was analyzed by FTIR spectroscopy with a Prestige-21 instrument, Shimadzu, Japan, by using the potassium bromide pellet technique. Overall, 10 mg of each sample were combined with 10 mg of solid KBr, and the mixture was subsequently pelletized with a vacuum pump. The spectra were measured between 400 and 4000 cm^{-1}. The morphology and particle size of the nanoparticles were analyzed using TEM (Hitachi Model H-7700, Ltd., Tokyo, Japan). The acceleration voltage was set at 100 kV, and the sample was dispersed in the solution using a sonicator. Next, a drop of sample was insulated on a plate, and the sample was observed at 50000x and 200000× magnification. The percentage of molecular components of nanoparticles were analyzed by SEM, coupled to an energy dispersive X-Ray (SEM-EDX) detector from Hitachi Model SU3500, Japan. The nanoparticles sample was placed on a carbon adhesive tape and treated with a gold (Au) coating using a power of 10 mA for 20 min. The measurement was set at the acceleration voltage of 10 kV with a 500× magnification. The crystal structure and phase purity of the synthesized nanoparticles were analyzed with an XRD Bruker D8 Advance, Germany.

2.2.3. Antibacterial assay

The potential antibacterial activity of the Nps in solution were determined with the agar well diffusion method [19]. *Staphylococcus aureus* ATCC 6538, *Bacillus subtilis* ATCC 6633, *Escherichia coli* ATCC 6539, and *Salmonella typhi* ATCC 8939 were used as model bacteria. A standard 0.5 McFarland suspension was used to test cultures that had been allowed to sit overnight and was prepared in Mueller Hinton Broth (MHB). First, the bacteria to be tested were inoculated into MHB and incubated at 37 °C and at a speed of 150 rpm in a shaker incubator. The bacterial suspension was subsequently diluted with saline solution until the optical density (OD) reached a range of 0.08–0.13 to achieve a 0.5 McFarland standard. Next, the 0.5 McFarland standardized bacterial suspensions were spread onto Mueller Hinton (MH) agar plates. Wells were made in the agar with the aid of a sterile cork borer, after which 100 μl of free rhamnolipid solution and dispersions of Nps were added. The plates were incubated at 37 °C for 24 h and the observed zones of

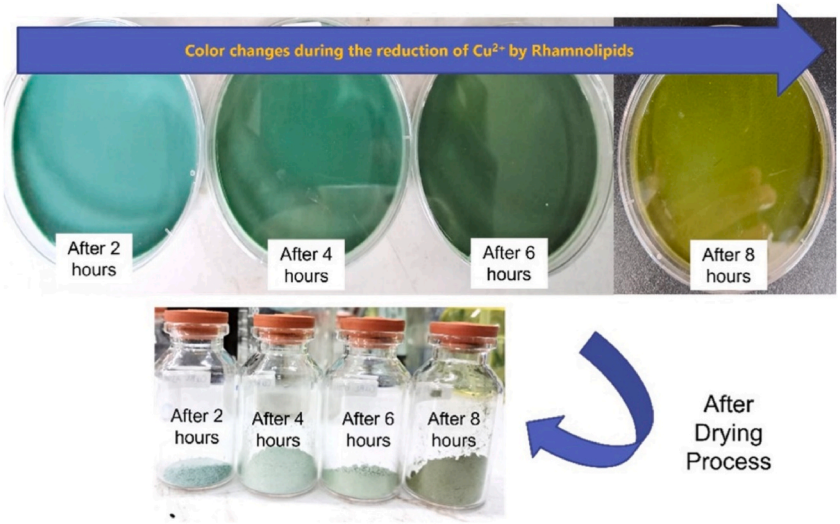

Fig. 1. Color changes during the reduction of Cu^{2+} ions by rhamnolipids.

inhibition were measured with a transparent metric ruler. The experiment was repeated three times.

The MIC and MBC were used to determine the minimum concentration of each sample that exhibited antibacterial activity against the bacteria tested, including *Staphylococcus aureus* ATCC 6538, *Bacillus subtilis* ATCC 6633, *Escherichia coli* ATCC 6539, and *Salmonella typhi* ATCC 8939, which were used as model bacteria. The testing process was carried out by following the procedures standardized by the Clinical and Laboratory Standard Institute (CLSI) [20]. The serial dilution of the nanoparticles and free rhamnolipid solutions were prepared with MHB in a 96-well microplate at an initial concentration of 10^4 μg/mL. The final population test of 8×10^5 CFU mL^{-1} was prepared by adding an overnight suspension culture of 0.5 McFarland standard to each well. The optical density was measured at 600 nm using a microplate reader after 18 h of incubation at 37 °C to inspect the bacterial growth. The lowest sample concentration without any discernible growth was expressed as the MIC. The wells with no apparent growth were inoculated onto MHB agar plates, and the plates were incubated for 24 h. The lowest concentration without any visible growth colonies of bacteria was expressed as the MBC.

3. Results and discussion

3.1. Synthesis of nanoparticles

Cu(I)-Rl Nps were synthesized by using a coprecipitation technique under 0.2 % NaOH alkaline conditions. The synthetic process was carried out at 100 °C under rotation with a Thermo Scientific magnetic stirring plate at a rotational speed of 1000 rpm for a total time of 8 h. Rhamnolipids act as reducing agent for Cu^{2+} ions in solution. The formation of nanoparticles was confirmed qualitatively from the color of the product formed, as shown in Fig. 1. The change in color over time demonstrated the reduction of Cu^{2+} ions by the rhamnolipid. In contrast, the synthesis of copper-based nanoparticles without the addition of a rhamnolipid showed no color changes over time after heating the solution to 100 °C. The free-copper-based rhamnolipid appears to form $Cu_2(OH)_3NO_3$ from the reactions of Cu^{2+} with OH^- (from NaOH) and has a light-blue color. The formation of nanoparticles was also confirmed by structural, elemental and crystalline analysis using FTIR, XRD and SEM-EDX.

The structure of Cu(I)-Rl Nps was analyzed using FTIR at 400-4000 cm^{-1}. Copper ions-based Nps, Rl, and $Cu(NO_3)_2.3H_2O$ were used as a comparison to observe the differences in the presence of the chemical bonds and functional groups in each product. The FTIR spectrum of the rhamnolipids is shown in Fig. 2. The FTIR spectrum of rhamnolipids in Fig. 2 shows a wide vibrational peak at 3391 cm^{-1}, indicating the –OH functional group in rhamnose. In the region of 2920 and 2859 cm^{-1}, a sharp peak was observed, indicating the presence of the C–H (–CH_2, –CH_3) functional group in the hydrocarbon chain of the rhamnolipids [21]. In addition, vibration peaks were also observed in the 1711 and 1405 cm^{-1} regions, indicating the presence of a carbonyl ester functional group (C═O). The stretching peak was also observed in the 1645 cm^{-1} region, representing the ester functional group. In the fingerprint area, there were peaks at 1051 cm^{-1}, which represents the presence of the ether functional group (C–O–C) of rhamnose, and at 825.62, 703.51, and 596.91 cm^{-1}, indicating the glycosidic linkage type in the rhamnolipid [22].

The FTIR spectrum of $Cu(NO_3)_2.3H_2O$ in Fig. 2 shows a wide vibrational peak at 3391 cm^{-1} which represents the free –OH functional group from the H_2O in $Cu(NO_3)_2.3H_2O$. In addition, a typical vibrational peak for $Cu(NO_3)_2.3H_2O$ was observed in the wavenumber region of 1618, 1378, and 831 cm^{-1}, indicating the presence of the N–O bond of Cu $(NO_3)_2.3H_2O$. As observed in the same figure, the synthesis of nanoparticles without the additions of rhamnolipid shows the formation of $Cu_2(OH)_3NO_3$. The peak at 3549 and 3444 cm^{-1} represents the free –OH and bound –OH groups from $Cu_2(OH)_3NO_3$ structures, whereas sharp peaks at the fingerprint area around 1400-600 cm^{-1} represent the Cu–O and N–O binding molecules [23]. The following reaction shows the formation of $Cu_2(OH)_3NO_3$:

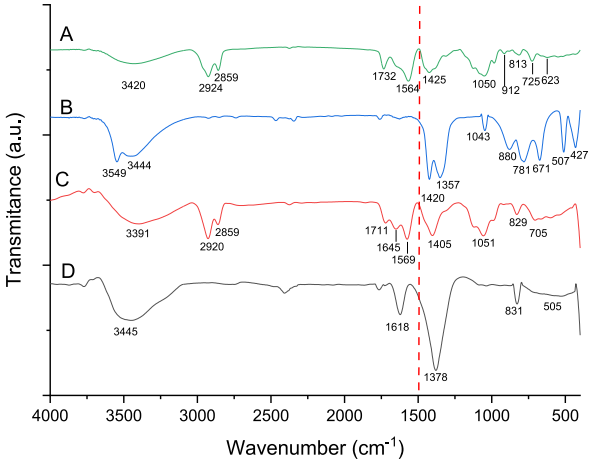

Fig. 2. FTIR Spectrum of Cu(I)-Rl Nps (A), copper ions-based Nps (B), rhamnolipids (C), $Cu(NO_3)_2.3H_2O$ (D).

$$2Cu(NO_3)_2 + 2NaOH + 2H_2O \rightarrow Cu_2(OH)_3NO_3 + 2NaNO_3 + H_3O^+ + NO_3^-$$

Moreover, the FTIR spectrum of Cu(I)-Rl Nps showed similar peaks as that of the FTIR spectrum of rhamnolipids and Cu $(NO_3)_2.3H_2O$. New peaks were also observed around 623 cm^{-1}, which indicates the formation of Cu(I)–O binding molecules from Cu (I)-Rl Nps.

The crystalline characteristics of Cu(I)-Rl Nps were also observed using X-ray diffraction (XRD) analysis. Fig. 3. A shows the XRD patterns of free rhamnolipid and Cu(I)-Rl Nps. The XRD spectrum of Cu(I)-Rl Nps shows several sharp peaks at $2\theta = 36.21°$, 42.23°, and 61,03° could be indexed to 111, 200, and 220 which shows the same result with the Cu_2O powder peaks obtained from of the International Centre of Diffraction Data card (JCPDS file no. 05–0667) [24]. The broader spectrum at $2\theta = 19.28°$ corresponds to the rhamnolipids. In comparison to XRD spectrum of Cu(I)-Rl Nps, all of the diffracted peaks in the XRD spectrum of copper ions-based Nps in Fig. 3. B can be indexed to monoclinic phase of $Cu_2(OH)_3NO_3$. [25].

The percentage of metal ions bound to rhamnolipids in Cu(I)-Rl Nps was also analyzed using EDS. The results in figure S1A showthat the elements contained in Cu(I)-Rl are carbon (C), oxygen (O), and copper (Cu). The carbon and oxygen atoms are representative of the rhamnolipid structure, while the Cu atom represented the copper attached to the rhamnolipids. The percentage mass of every atom present in the nanoparticle system was 61.17 %, 21.09 %, and 17.75 % for carbon, oxygen, and copper atoms respectively. In comparison, figure S1.Bshows that the percentage mass of every atom present in copper ions-based Nps was 11.48 % nitrogen, 34.13 % oxygen and 54.39 % copper. This result is also confirm the formation of $Cu_2(OH)_3NO_3$.

3.2. Interactions between rhamnolipids and metal ions

Fig. 4 shows the possible interactions between Cu ions and rhamnolipids. Under alkaline conditions, the carboxylic acid (–COOH) functional group of the rhamnolipid deprotonates to become $–COO^-$. Furthermore, the rhamnolipid reduces the Cu^{2+} ion to Cu^+ in solution. Two possible mechanisms for the formation of nanoparticles Cu (I)-Rl are available (as seen in Fig. 4. A). The first involves electrostatic interactions between negatively charged carbocylic acid group in rhamnolipids and positively charged Cu^+ metal ions. The formation of this interaction is marked by a shift in the peak of the rhamnolipid FTIR spectrum band in the wavenumber region of 1710–1780 cm^{-1}, indicating a change in the characterization of the carboxylic group in the rhamnolipid structure. In the second mechanism, the rhamnolipids function as ligands that form complexes with Cu^+ metal ions. The formation of this interaction is confirmed by XRD and FTIR result which shown the formation of Cu(I)–O binding molecules.

Research regarding geometric models related to the interaction of rhamnolipids with various metal ions (Ca, Ag, Cu and Al) has been carried out by Korni et al. (2017) using the density functional theory (DFT) method. The result shows that there are 3 possible conformations between rhamnolipid and cationic metal ions. First, the negatively charged of the deprotonated carboxylic acid functional group from rhamnolipid interact with cationic metal ions through ionic bond. Another possible conformation is the formation of a bi-coordination complex between oxygen atoms of the ester and alkoxy groups in rhamnolipids with the metal ion. Lastly, a tri-coordinates complex was formed between two oxygen atoms from the ester and alkoxy groups of rhamnolipid with the metal ions [26].

3.3. Characterizations of nanoparticles

The synthesized Cu(I)-Rl Nps were subsequently characterized to better understand the physiochemical properties of Cu(I)-Rl Nps compared to copper ions-based Nps and rhamnolipid. The characterization carried out was morphological analysis using TEM, surface charge analysis using ZPA, molecular size distribution analysis using PSA and nanoparticle dispersion stability at various pH using

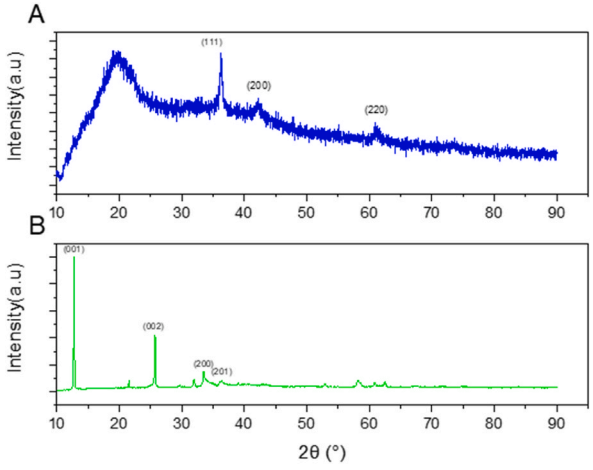

Fig. 3. XRD pattern of Cu(I)-Rl Nps (A) and copper ions-based Nps (B).

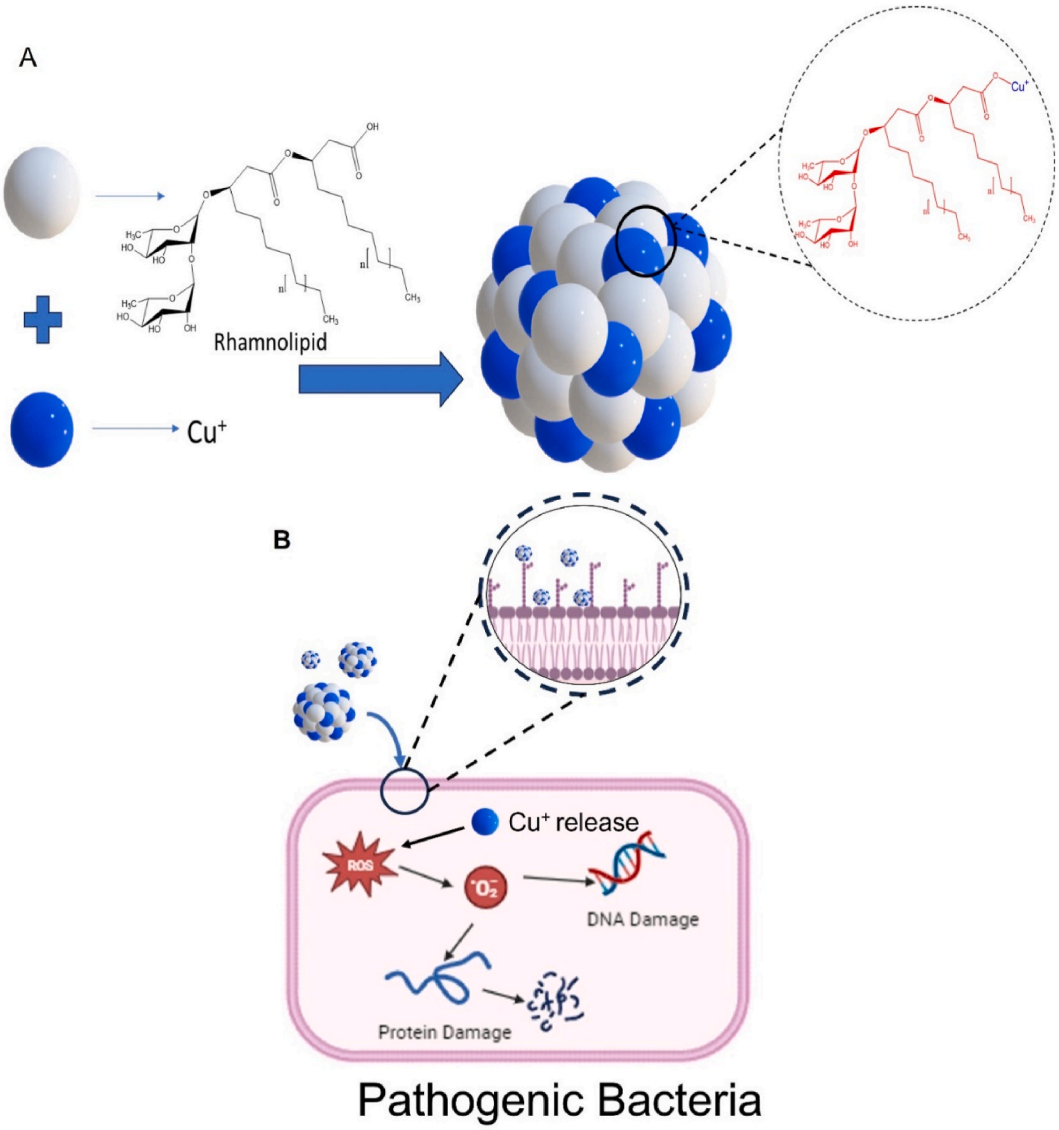

Fig. 4. Interactions between Rhamnolipid with Cu^{+} (A) and the mechanism of the antibacterial effects of Cu(I)-Rl on the bacterial cell (B).

UV–Vis Spectrophotometry.

The TEM results in Fig. 5. A-B show that Cu(I)-Rl Nps have a spherical shape. As shown in Fig. 5. A, a darker area represents copper ion nanoparticles surrounded by rhamnolipid on the surface. In comparison, Fig. 5. C-D shows that the shape of copper ions-based Nps is more irregular and displays a tendency to form aggregates.

In the Cu(I)-Rl Nps system, the rhamnolipid acts as a capping agent, which could prevent nanoparticle aggregation. This property is further demonstrated by measurements of the size distribution and zeta potential, as shown in Table S1.

The zeta potential quantifies the electrostatic repulsion or attraction between particles. Therefore, zeta potensial is the most accurate indication of the stability of dispersions. Either negative or positive zeta potential levels should be obtained in order to prevent particle aggregation due to electrostatic repulsion between individual particles [27]. In general, a zeta potential value greater than ± 30 mV is considered to have sufficient repulsive force to achieve increased physical colloidal stability [28]. As shown in Table S1, copper ions-based Nps in aqueous solution have a zeta potential value of 17.2 ± 1.6 mV, which leads to faster aggregation compared to Cu(I)-Rl Nps, which has a zeta potential of -30.0 ± 1.0 mV. Moreover, the negative charge of Cu(I)-Rl Nps in aqueous solution supports the TEM finding that the proportion of rhamnolipid is in the surface of the nanoparticles caused by negatively charged rhamnolipid, as shown in Table S1.

As another observation, the particle size of Cu(I)-Rl Nps appears to be smaller than that of copper ions-based Nps. The rhamnolipid can act as stabilizer and surface coating for Cu(I) in solutions. Surfactants bind to metal nanoparticles on the surface and prevent particle aggregation and oxidation by increasing the repulsion between the particles, thereby leading to smaller sized nanoparticles.

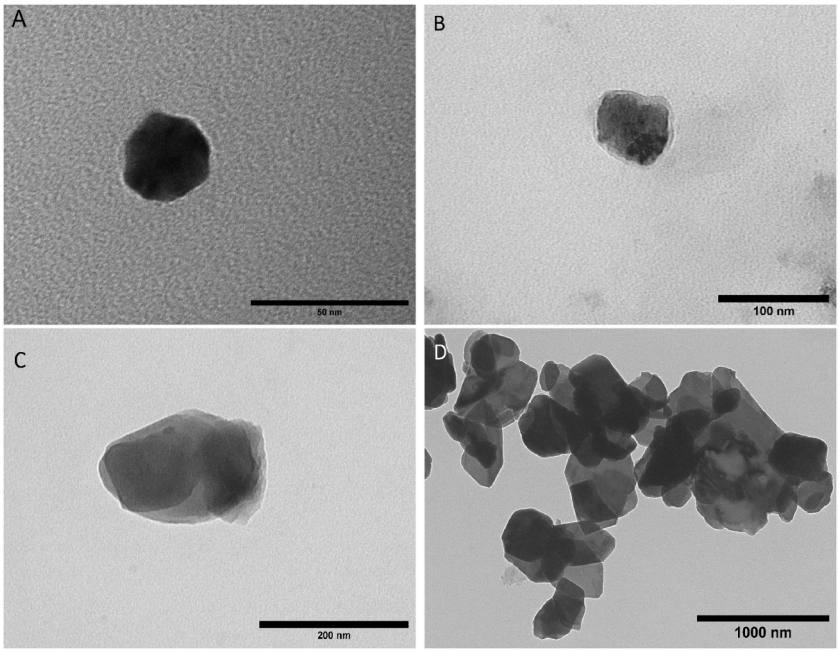

Fig. 5. TEM imaging result of Cu(I)-Rl Nps (A–B), copper ions-based Nps (C) and aggregations of copper ions-based Nps (D).

Moreover, the pH conditions of the dispersing environment appear to influence the stability of Cu(I)-Rl Nps dispersions. As shown in Fig. S1, Cu(I)-Rl Nps precipitates faster under acidic (pH 5) and alkaline (pH 8–9) conditions than under neutral ones. Under neutral conditions (pH 6–7), the dispersion of Cu(I)-Rl Nps was stable under neutral conditions for a period of 3 h.

3.4. Antibacterial activity

The agar well diffusion method was utilized to determine the antibacterial activity of Cu(I)-Rl Nps, copper ions-based Nps, and rhamnolipids. Each antibacterial agent was administered at a concentration of 10^4 μg/mL, and their antibacterial activity was tested against *Staphylococcus aureus* ATCC 6538, *Bacillus subtilis* ATCC 6633, *Escherichia coli* ATCC 6539, and *Salmonella typhi* ATCC 8939. Antibacterial activity was assessed by the diameter of the bacterial inhibition zone caused by the antibacterial agents.

As shown in Table 1, high concentrations of Cu(I)-Rl Nps exhibited antibacterial activity against *Staphylococcus aureus* ATCC 6538, *Bacillus subtilis* ATCC 6633, *Escherichia coli* ATCC 6539, and *Salmonella typhi* ATCC 8939. Cu(I)-Rl Nps showed the most potent antimicrobial activity against *Bacillus subtilis* ATCC 6633. In comparison to Cu(I)-Rl Nps, the rhamnolipid at high concentrations showed antibacterial activity against *Staphylococcus aureus* ATCC 6538 and *Bacillus subtilis* ATCC 6633. These results indicate wider inhibition zone than rhamnolipid-based silver nanoparticles from previous studies by Bharali et al. (2013) [17]. Another observation on *Escherichia coli* ATCC 6539, or *Salmonella typhi* ATCC 8939 shows no inhibition zone from Cu(I)- Rl Nps. In contrast, copper ions-based Nps showed antibacterial activity only against *Bacillus subtilis* ATCC 6633.

Further investigations of the antibacterial activity of Cu(I)-Rl Nps compared to copper ions-based Nps and rhamnolipid were carried out by determining the MIC and MIB values. MIC is defined as the lowest concentration of an antimicrobial agent that will inhibit visible microbial growth during overnight incubation, and MBC is defined as the minimum concentration of an antimicrobial agent that can kill bacteria [29]. The MIC and MBC results are shown in Table 2. Based on the results depicted in Table 2. Cu(I)-Rl Nps demonstrated enhanced antibacterial activity against *Bacillus subtilis* and *Escherichia coli*. Testing against *Staphylococcus aureus* revealed that free rhamnolipid exhibited greater antibacterial activity than Cu(I)-Rl Nps and had lower MIC and MBC values compared to Cu(I)-Rl Nps, which supports this observation. In further experiments, Cu(I)-Rl Nps demonstrated insufficient antibacterial activity against *Salmonella typhi*.

Table 1
Sensitivity test of rhamnolipid, copper ions-based Nps and Cu(I)-Rl Nps using the Well Diffusions Method.

Tested Bacteria	*Bacillus subtilis* ATCC 6633	*Staphylococcus aureus* ATCC 6538	*Escherichia coli* ATCC 6539	*Salmonella typhi* ATCC 8939
	Inhibition Zone Diameters (mm)			
Rhamnolipids	28.3 ± 2.8	27.3 ± 4.1	0	0
Copper ions-based Nps	34.3 ± 2.1	0	0	0
Cu(I)-Rl Nps	36.7 ± 1.5	31.3 ± 5.0	18.3 ± 2.9	14.7 ± 2.3

Table 2
MIC and MBC of rhamnolipids, Cu(I)-Rl Nps and copper ions-based Nps.

Antibacterial Agents	*Bacillus subtilis* ATCC 6633		*Staphylococcus aureus* ATCC 6538		*Escherichia coli* ATCC 6539		*Salmonella typhi* ATCC 8939	
	MIC (μg/mL)	MBC (μg/mL)	MIC (μg/mL)	MBC (μg/mL)	MIC (μg/mL)	MBC (μg/mL)	MIC (μg/mL)	MBC (μg/mL)
Rhamnolipids	62	62	19	19	>2000	>2000	>5000	>5000
Copper ions-based Nps	1250	2500	5000	5000	2500	2500	>5000	>5000
Cu(I)-Rl Nps	19	19	78	78	78	78	2500	2500
$Cu(NO_3)_2$. $3H_2O$	1250	1250	1250	1250	2500	2500	5000	5000

The combined antibacterial effect of Cu metal ions and rhamnolipids in the nanoparticle system was also studied by calculating the fractional inhibitory concentration (FIC). The FIC index is calculated by using the MIC of the antimicrobial compound alone and the respective MIC of the compounds when combined [30]. In the present study, the FIC index was determined by using the formula in Equation (1):

$$\sum FIC = \frac{MIC\ of\ Rl\ in\ nanoparticles}{MIC\ of\ Free\ Rl} + \frac{MIC\ of\ Cu\ ions\ in\ nanoparticles}{MIC\ of\ Free\ Cu\ ions} \quad (1)$$

Combined antimicrobial interactions were classified with the following parameters: when the FIC index was 0.5, the interactions were synergistic; when the FIC index was between 0.5 and 4, the interactions were indifferent; and when the FIC index was greater than 4, the interactions were antagonistic [31]. The FIC of each material used in the present study is shown in Table S2. Based on the results in Table S2, the combination of rhamnolipids and metal ions as nanoparticle has a synergistic effect on *Bacillus subtilis* ATCC 6633 and *Escherichia coli* ATCC 6533.

3.5. Mechanism of antibacterial activity of Cu(I)-Rl Nps

The antibacterial mechanism of action of Cu(I)-Rl requires further study. However, the results of our literature review suggest that the combination of rhamnolipids and Cu metal ions can produce a synergistic effect on their antibacterial activity, particularly against *Bacillus subtilis* and *Escherichia coli*. The combined effects of Cu(I) metal ions and rhamnolipids may account for the increased antibacterial activity of Cu(I)-Rl. The overall process is illustrated in Fig. 4. B. Rhamnolipids interact with bacterial cells in three different ways [32]. First, rhamnolipids alter the surface charge of bacterial cells by neutralizing them, increasing their surface charge, or interacting with functional groups on the surface of the bacterial cell membrane. Second, rhamnolipids increase cell permeability and trigger the release of the constituents of the cell's components and increase the number of Cu(I) Nps that enter the cells. Third, rhamnolipids cause the release of molecular components directly on the cell surface that affect their surface charge. This process is capable of directly triggering bacterial cell death. In other route, the copper ions-based Nps or Cu ions that enter the interior of the cell after being released from the nanoparticle system can induce the production of reactive oxygen species (ROS), which may effects cell mortality via oxidative stress by destroying crucial molecular components that are necessary for the metabolic processes of bacteria [33].

ROS such as superperoxide anion ($O_2^{\bullet-}$), hydrogen peroxide (H_2O_2) and hydroxyl radicals ($HO^{\bullet}$) are generally produced in the process of metabolic respiration. H_2O_2 is classified as a non-radical oxygen species due to its chemical stability. In contrast, superoxide and hydroxy radicals are categorized as free radical oxygen species which have short half-life time at 37 °C which is around 10^{-6} s and 10^{-9} s respectively [34]. Their levels are controlled through several enzymatic pathways involving superoxide dismutase (SOD) and catalase [35]. However, the presents of Cu ions or Cu Nps could increase the ROS concentration and leads to apoptosis process of cell caused by oxidative stress. The mechanism of ROS generation by Cu species usually involves redox reactions involving the oxidation process of Cu Nps to Cu^{2+} and resulted in H_2O_2 as byproduct which leads to membran damage of cell [5]. Moreover the release of Cu^{2+} in the cell leads to generations of superoxide. Consequently, protonation of superoxide resulted in hydroxyl-radical formation. Hydroxyl-radicals are highly reactive compared to other oxygen-free radical species which caused DNA damage in cells of all types [36].

Other research related to the mechanism of antibacterial activity of Cu nanoparticles shows the influence of the particle size distribution. Research by Apllerot et al. (2012) showed that CuO Nps with a size of 2 nm had higher antibacterial activity compared to CuO Nps with a size of more than 800 nm. Additional investigation revealed that the utilization of smaller nanoparticle sizes led to elevated concentrations of superoxide anions, subsequently inducing higher oxidative stress to the cell [37]. This study had similar result, which shown that Cu(I)-Rl Nps with smaller size show higher antibacterial activity compare to copper ions-based Nps which has larger particles size. In addition to the nanoparticle size, the antibacterial activity of Cu(I)-Rl Nps can also be impacted by the shape of the nanoparticles. An improvement in the antibacterial activity was observed in spherical Cu(I)-Rl Nps compared to irregular copper ions-based Nps. Similar findings were found in a previous study by Laha et al. (2014), which found that spherical CuO nanoparticles had better antibacterial activity than nanosheets of CuO against the Gram-negative bacteria *Proteus vulgaris* and *E. coli*. Nevertheless, additional investigation reveals that spherical CuO are less effective than Cu nanosheets against the Gram-positive bacteria *Bacillus subtilis* and *Micrococcus luteous* [38].

Other factor that may contribute to the antibacterial mechanism of action of nanoparticles is the difference in cell wall structural

components between Gram-negative and Gram-positive bacteria [39]. The Cu(I)-Rl NPs exhibited better antibacterial activity against the Gram-positive bacteria *Bacillus subtilis* in comparison to Gram-negative bacteria *Escherichia coli*. The Cu(I)-Rl Nps has smaller MIC value against *Bacillus subtilis* (19 μg/mL) than against *Escherichia coli* (78 μg/mL). As Cu(I)-Rl Nps have more negative zeta potensial in comparison to copper ions-based Nps. It is sugested that rhamnolipid is located in on the surface of the nanoparticles which is resulted in different antibacterial activity againts Gram-negative and Gram-positive bacteria. According to other studies, it has been proposed that rhamnolipids exhibit greater efficacy against Gram-positive bacteria compared to Gram-negative bacteria due to the presence of an outer membrane in Gram-negative bacteria, which can potentially impede the penetration of biosurfactant molecules [40].

4. Conclusions

Our findings demonstrate a green synthesis methods of functionalized copper ions based nanoparticles with biosurfactant rhamnolipid as reducing and capping agents. The addition of rhamnolipids onto the nanoparticle system results in smaller and more uniformly sized nanoparticles compared to copper ions-based Nps without the addtions of rhamnolipids. The results of the characterization of the nanoparticle system support the findings of this analysis. The combination of both materials also shows a synergistic effect on their antibacterial activity againts *Bacillus subtilis* and *Escherichia coli*. The improvement of these activity can be attributed to a combination of antibacterial effects from each material. Rhamnolipids present on the surface of the nanoparticles operate by altering the structural components and electric charge of the bacterial cell, which increases insertion of copper ions-based Nps and copper ions into the bacterial cells. This process can induce cell apoptosis by producing ROS. Although further research regarding the antibacterial mechanism of Cu(I)-Rl still needs to be done. The findings of the current study indicate that Cu(I)-Rl has the potential to serve as an alternative sustainable antibacterial agent for combatting the growing problem of bacterial resistance to currently available antibacterial agents.

CRediT authorship contribution statement

Fera Faridatul Habibah: Conceptualization, Formal analysis, Investigation, Methodology, Validation, Writing - original draft, Writing - review & editing, Data curation. **Wa Ode Sri Rizki:** Investigation, Methodology, Writing - review & editing, Data curation, Conceptualization. **Atthar Luqman Ivansyah:** Formal analysis, Validation, Writing - original draft, Writing - review & editing. **Dea Indriani Astuti:** Formal analysis, Supervision, Validation, Writing - review & editing. **Rukman Hertadi:** Conceptualization, Data curation, Formal analysis, Funding acquisition, Supervision, Validation, Writing - original draft, Writing - review & editing.

Declaration of competing interest

The authors declare that they have no known competing financial interests or personal relationships that could have appeared to influence the work reported in this paper.

Acknowledgements

This work is funded by a grant from the Penelitian, Pengabdian Masyarakat, dan Inovasi (PPMI) Program in 2020 by Bandung Institute of Technology, Indonesia with contract number: 120/IT1.C02/SK-TA/2023.

Appendix A. Supplementary data

Supplementary data to this article can be found online at https://doi.org/10.1016/j.heliyon.2024.e24242.

References

[1] S. Doron, L. Gorbach, Bacterial Infections: Overview, International Encyclopedia of Public Health, 2008, pp. 273–282, https://doi.org/10.1016/B978-012373960-5.00596-7.
[2] M. Lobanovska, G. Pilla, Penicillin's discovery and antibiotic resistance: Lessons for the Future? Yale J. Biol. Med. 90 (2017) 135–145.
[3] E. Peterson, P. Kaur, Antibiotic resistance mechanisms in bacteria: relationships between resistance determinants of antibiotic producers, environmental bacteria, and clinical pathogens, Front. Microbiol. 9 (2018), https://doi.org/10.3389/fmicb.2018.02928.
[4] E. Sánchez-López, D. Gomes, G. Esteruelas, L. Bonilla, A.L. Lopez-Machado, R. Galindo, et al., Metal-based nanoparticles as antimicrobial agents: an overview, Nanomaterials 10 (2020), https://doi.org/10.3390/nano10020292.
[5] M.L. Ermini, V. Voliani, Antimicrobial nano-agents: the copper age, ACS Nano 15 (2021) 6008–6029, https://doi.org/10.1021/acsnano.0c10756.
[6] D. Franco, G. Calabrese, S.P.P. Guglielmino, S. Conoci, Metal-based nanoparticles: antibacterial mechanisms and biomedical application, Microorganisms 10 (2022), https://doi.org/10.3390/microorganisms10091778.
[7] K. Ahlawat, R. Jangra, S. Chaturvedi, C. Prakash, A. Dixit, D. Fulwani, et al., Photocatalytic oxidation conveyor "pCOC" system for large scale surface disinfection, Rev. Sci. Instrum. 93 (2022), https://doi.org/10.1063/5.0082222.
[8] M.L. Ermini, V. Voliani, Antimicrobial nano-agents: the copper age, ACS Nano 15 (2021) 6008–6029, https://doi.org/10.1021/acsnano.0c10756.
[9] B. Das, S. Patra, Antimicrobials: meeting the challenges of antibiotic resistance through nanotechnology, in: Nanostructures for Antimicrobial Therapy: Nanostructures in Therapeutic Medicine Series, Elsevier, 2017, pp. 1–22, https://doi.org/10.1016/B978-0-323-46152-8.00001-9.

[10] M.B. Gawande, A. Goswami, F.X. Felpin, T. Asefa, X. Huang, R. Silva, et al., Cu and Cu-based nanoparticles: synthesis and applications in catalysis, Chem Rev 116 (2016) 3722–3811, https://doi.org/10.1021/acs.chemrev.5b00482.
[11] M.S. Aguilar, R. Esparza, G. Rosas, Synthesis of Cu nanoparticles by chemical reduction method, Trans. Nonferrous Metals Soc. China 29 (2019) 1510–1515, https://doi.org/10.1016/S1003-6326(19)65058-2.
[12] L. Kvítek, A. Panáček, J. Soukupová, M. Kolář, R. Večeřová, R. Prucek, et al., Effect of surfactants and polymers on stability and antibacterial activity of silver nanoparticles (NPs), J. Phys. Chem. C 112 (2008) 5825–5834, https://doi.org/10.1021/jp711616v.
[13] C.B.B. Farias, A.F. Silva, R.D. Rufino, J.M. Luna, J.E. Gomes Souza, L.A. Sarubbo, Synthesis of silver nanoparticles using a biosurfactant produced in low-costmediumas stabilizing agent, Electron. J. Biotechnol. 17 (2014) 122–125, https://doi.org/10.1016/j.ejbt.2014.04.003.
[14] A.M. Abdel-Mawgoud, F. Lépine, E. Déziel, Rhamnolipids: diversity of structures, microbial origins and roles, Appl. Microbiol. Biotechnol. 86 (2010) 1323–1336, https://doi.org/10.1007/s00253-010-2498-2.
[15] T.B. Lotfabad, F. Shahcheraghi, F. Shooraj, Assessment of antibacterial capability of rhamnolipids produced by two indigenous Pseudomonas aeruginosa strains, Jundishapur J. Microbiol. 6 (2013) 29–35, https://doi.org/10.5812/jjm.2662.
[16] C.A. Marangon, V.C.A. Martins, M.H. Ling, C.C. Melo, A.M.G. Plepis, R.L. Meyer, et al., Combination of rhamnolipid and chitosan in nanoparticles boosts their antimicrobial efficacy, ACS Appl. Mater. Interfaces 12 (2020) 5488–5499, https://doi.org/10.1021/acsami.9b19253.
[17] P. Bharali, J.P. Saikia, S. Paul, B.K. Konwar, Colloidal silver nanoparticles/rhamnolipid (SNPRL) composite as novel chemotactic antibacterial agent, Int. J. Biol. Macromol. 61 (2013) 238–242, https://doi.org/10.1016/j.ijbiomac.2013.07.006.
[18] R. Hertadi, M.M.S. Amari, E. Ratnaningsih, Enhancement of antioxidant activity of levan through the formation of nanoparticle systems with metal ions, Heliyon 6 (2020), https://doi.org/10.1016/j.heliyon.2020.e04111.
[19] M. Balouiri, M. Sadiki, S.K. Ibnsouda, Methods for in vitro evaluating antimicrobial activity: a review, J Pharm Anal 6 (2016) 71–79, https://doi.org/10.1016/j.jpha.2015.11.005.
[20] Clinical and Laboratory Standards Institute (CLSI), Methods for Dilution Antimicrobial Susceptibility Tests for Bacteria that Grow Aerobically, vol. 11, Clinical and Laboratory Standards Institute, 2018, p. 92.
[21] K.V. Deepika, M. Raghuram, P.V. Bramhachari, Rhamnolipid biosurfactant production by Pseudomonas aeruginosa strain KVD-HR42 isolated from oil contaminated mangrove sediments, Afr. J. Microbiol. Res. 11 (2017) 218–231, https://doi.org/10.5897/ajmr2015.7881.
[22] R. Khademolhosseini, A. Jafari, S.M. Mousavi, H. Hajfarajollah, K.A. Noghabi, M. Manteghian, Physicochemical characterization and optimization of glycolipid biosurfactant production by a native strain of Pseudomonas aeruginosa HAK01 and its performance evaluation for the MEOR process, RSC Adv. 9 (2019) 7932–7947, https://doi.org/10.1039/C8RA10087J.
[23] Y. Zhan, X. Zhou, B. Fu, Y. Chen, Catalytic wet peroxide oxidation of azo dye (Direct Blue 15) using solvothermally synthesized copper hydroxide nitrate as catalyst, J. Hazard Mater. 187 (2011) 348–354, https://doi.org/10.1016/j.jhazmat.2011.01.027.
[24] Y. Yang, D. Xu, Q. Wu, P. Diao, Cu2O/CuO bilayered composite as a high-efficiency photocathode for photoelectrochemical hydrogen evolution reaction, Sci. Rep. 6 (2016), https://doi.org/10.1038/srep35158.
[25] A. Pendashteh, M.S. Rahmanifar, M.F. Mousavi, Morphologically controlled preparation of CuO nanostructures under ultrasound irradiation and their evaluation as pseudocapacitor materials, Ultrason. Sonochem. 21 (2014) 643–652, https://doi.org/10.1016/j.ultsonch.2013.08.009.
[26] S.A. Kornii, V.I. Pokhmurs'kyi, V.I. Kopylets, I.M. Zin, N.R. Chervins'ka, Quantum-chemical analysis of the electronic structures of inhibiting complexes of rhamnolipid with metals, Mater. Sci. 52 (2017) 609–619, https://doi.org/10.1007/s11003-017-9998-5.
[27] V. Selvamani, Stability Studies on Nanomaterials Used in Drugs. Characterization and Biology of Nanomaterials for Drug Delivery: Nanoscience and Nanotechnology in Drug Delivery, Elsevier, 2018, pp. 425–444, https://doi.org/10.1016/B978-0-12-814031-4.00015-5.
[28] M. Gumustas, C.T. Sengel-Turk, A. Gumustas, S.A. Ozkan, B. Uslu, Effect of polymer-based nanoparticles on the assay of antimicrobial drug delivery systems, in: Multifunctional Systems for Combined Delivery, Biosensing and Diagnostics, Elsevier, 2017, pp. 67–108, https://doi.org/10.1016/B978-0-323-52725-5.00005-8.
[29] M.E. Levison, Pharmacodynamics of antimicrobial drugs, Infect Dis Clin North Am 18 (2004) 451–465, https://doi.org/10.1016/j.idc.2004.04.012.
[30] L. Magalhães, M. Nitschke, Antimicrobial activity of rhamnolipids against Listeria monocytogenes and their synergistic interaction with nisin, Food Control 29 (2013) 138–142, https://doi.org/10.1016/j.foodcont.2012.06.009.
[31] N.A. Alshaikh, K. Perveen, A.H. Bahkali, Effect of silver nanoparticles alone and in combination with fluconazole on Candida albicans, J. King Saud Univ. Sci. 35 (2023), https://doi.org/10.1016/j.jksus.2022.102399.
[32] B. Shao, Z. Liu, H. Zhong, G. Zeng, G. Liu, M. Yu, et al., Effects of rhamnolipids on microorganism characteristics and applications in composting: a review, Microbiol. Res. 200 (2017) 33–44, https://doi.org/10.1016/j.micres.2017.04.005.
[33] S. Mahmoodi, A. Elmi, S. Hallaj Nezhadi, Copper nanoparticles as antibacterial agents, J Mol Pharm Org Process Res 6 (2018), https://doi.org/10.4172/2329-9053.1000140.
[34] C.P. Rubio, J.J. Cerón, Spectrophotometric assays for evaluation of Reactive Oxygen Species (ROS) in serum: general concepts and applications in dogs and humans, BMC Vet. Res. 17 (2021), https://doi.org/10.1186/s12917-021-02924-8.
[35] A.J. Kowaltowski, N.C. de Souza-Pinto, R.F. Castilho, A.E. Vercesi, Mitochondria and reactive oxygen species, Free Radic. Biol. Med. 47 (2009) 333–343, https://doi.org/10.1016/j.freeradbiomed.2009.05.004.
[36] V.I. Lushchak, Classification of oxidative stress based on its intensity, EXCLI J 13 (2014).
[37] G. Applerot, J. Lellouche, A. Lipovsky, Y. Nitzan, R. Lubart, A. Gedanken, et al., Understanding the antibacterial mechanism of CuO nanoparticles: revealing the route of induced oxidative stress, Small 8 (2012) 3326–3337, https://doi.org/10.1002/smll.201200772.
[38] D. Laha, A. Pramanik, A. Laskar, M. Jana, P. Pramanik, P. Karmakar, Shape-dependent bactericidal activity of copper oxide nanoparticle mediated by DNA and membrane damage, Mater. Res. Bull. 59 (2014) 185–191, https://doi.org/10.1016/j.materresbull.2014.06.024.
[39] A. Mai-Prochnow, M. Clauson, J. Hong, A.B. Murphy, Gram positive and Gram negative bacteria differ in their sensitivity to cold plasma, Sci. Rep. 6 (2016), https://doi.org/10.1038/srep38610.
[40] A.V. Sotirova, D.I. Spasova, D.N. Galabova, E. Karpenko, A. Shulga, Rhamnolipid-biosurfactant permeabilizing effects on gram-positive and gram-negative bacterial strains, Curr. Microbiol. 56 (2008) 639–644, https://doi.org/10.1007/s00284-008-9139-3.